KSME

Springer

Journal of Mechanical Science and Technology 35 (4) 2021

Original Article
DOI 10.1007/s12206-021-0323-8

Keywords:
· Health index
· Liquid filtration filter
· LSTM
· PHM
· Remaining useful life

Correspondence to:
Janghyeok Yoon
janghyoon@konkuk.ac.kr

Citation:
Lee, S., Lee, S., Lee, K., Lee, S., Chung, J., Kim, C.-W., Yoon, J. (2021). Data-driven health condition and RUL prognosis for liquid filtration systems. Journal of Mechanical Science and Technology 35 (4) (2021) 1597~1607.
http://doi.org/10.1007/s12206-021-0323-8

Received August 25th, 2020
Revised November 26th, 2020
Accepted December 24th, 2020

† Recommended by Editor Seungjae Min

Data-driven health condition and RUL prognosis for liquid filtration systems

Seunghyun Lee[1], Seungju Lee[1], Kwonneung Lee[1], Sangwon Lee[1], Jaemin Chung[1], Chang-Wan Kim[2] and Janghyeok Yoon[1]

[1]Department of Industrial Engineering, Konkuk University, Seoul 05029, Korea, [2]School of Mechanical Engineering, Konkuk University, Seoul 05029, Korea

Abstract Because the clogging of filters leads to degradation and failure of mechanical systems, it is important to assess the health condition of a filter and predict its remaining useful life (RUL). Despite prior studies of liquid filtration systems, adequate attention has not been paid to data-driven health condition and RUL prognosis. Therefore, this study suggests a data-driven prognosis approach for liquid filtration systems. We define a health index (HI) for the filter under study and then predict HI values from the degradation point to the end-of-life using recurrent neural network algorithms, thereby yielding the filter's RUL. As a result, the bidirectional LSTM achieved the best performance, and the RUL measured through HI prediction was close to the actual RUL. The proposed approach can be used for the maintenance of liquid filtration systems in various industries.

1. Introduction

Filters are used for the removal of contaminants from fluids in a variety of industries, such as aviation and power plants. Because filters support a smooth operation of various systems, they are considered to be a significant maintenance factor [1]. As a fluid passes through a filter, contaminants become trapped in the filter. Over time, such contaminants can block the filter, thereby leading to degradation and failure of a machine [2]. Thus, for mechanical system managers, preventive maintenance, replacing old equipment or parts before they clog, is very important. Condition-based maintenance (CBM) can be selected as a way of preventive maintenance. CBM assesses the health of the system based on data collected from the system through continuous monitoring or inspection to determine the required maintenance before a predicted failure [3]. Therefore, for the efficient maintenance of mechanical systems, it is important to reflect the CBM in order to assess the current health condition of a filter through real-time monitoring and predict the remaining useful life (RUL) of the filter [4].

The most commonly used CBM method is prognostics and health management (PHM). PHM is a field of engineering with great potential to improve machine reliability, reduce maintenance costs [5] and numerically evaluates the health condition of a mechanical system [6]. PHM aims to achieve high availability at minimal cost by providing methods and tools to design optimal maintenance policies for specific assets under unique operational and performance degradation conditions [7]. Overall, the PHM can be divided into four areas: detection, diagnostics, assessment, and prognostics [8]. Detection aims to identify failures in the engineering system without knowing the root cause. Diagnosis aims to find out the causes of the detected failures, so that corrective measures can be arranged. Furthermore, the specific failure type of detected failure can be found out through diagnosis. Assessment aims to evaluate the health state of machine or equipment based on its recent motions. Assessment is often used to illustrate the machine degradation process when estimating the life of a machine. Prognosis mainly predicts the future health states and the RUL of the system. Among them, failure prognostics is an important area in the PHM [9].

Khelif et al. [10] reported that a prognostics model can be divided into physics-based and

data-driven models. Physics-based models mathematically describe the condition of a product using knowledge of various failures that may occur in the equipment [11], thereby making them more accurate in failure prognostics than the other models [12]. Therefore, physics-based models are suitable for industries such as power plants and aircraft where safety is a top priority. However, physics-based models can be difficult to link with real-time data [13]. Moreover, their universal usability is limited due to the requirement of expertise for each product and consumption of numerous resources [14].

Data-driven models provide predictions of equipment failure mechanisms based on the collected data [15]. With the advancement of sensor technology, various types of data can be collected in real-time from the products currently in use. In addition, as data becomes more vast, various analytical techniques continue to emerge. For these reasons, research into data-driven models is actively being conducted, and thus, the accuracy of the data-driven models in RUL estimation is increasing. For example, Niuhic et al. [16] used a support vector machine to estimate the health and RUL of lithium-ion batteries. In addition, Skaf et al. [17] used the state-based prognostics with duration method to estimate the RUL of a filter. Furthermore, Ho et al. [18] used an autoregressive integrated moving average and recurrent neural network (RNN) to predict the failure point of a compressor.

Although studies on PHM have been conducted in various fields, filter-related research remains insufficient. First, a liquid filter (liquid filtration filter) is important, which can solve various problems such as maintaining the purity of the oil and resolving water shortages [19]. However, studies on liquid filters have been insufficient than that on other filter types. Second, most of previous studies on liquid filters have used a physics-based model. Physics-based models are frequently used in failure prognostics studies, but it is expensive to implement them, and it may be difficult to create accurate models in complex systems. Therefore, studies on data-driven failure prognostics can be conducted to develop efficient predictive models using the given data. Third, to predict the RUL, prior studies on failure prognostics have generally predicted the indicator itself, which has a high correlation with the system. This approach requires knowledge of various indicators, making it difficult for non-experts to understand the current state of a system. A health index (HI) is a quantitative indicator of the overall health condition of the system, and simply indicates the state with a value between 0 and 1 through combines components of the system [20]. Consequently, efficient HI-based condition assessment and failure prognostics studies are required.

This study defines and predicts the HI for a liquid filter using a data-driven model, consecutively deriving the RUL of the filter. The data used in this study were collected through sensors and provided by the PHMe20 Data Challenge (http://phmeurope.org/2020/data-challenge-2020). To estimate the RUL, the degradation point of the system performance must be first measured [21]. Accordingly, K-means clustering was used for the collected data to identify the performance degradation point of the filter. Next, long-short term memory (LSTM) was used to estimate the RUL of the filter. To increase the validity of the analysis, the results were analyzed by dividing LSTM approaches into vanilla, stacked, and bidirectional LSTM. Furthermore, various metrics, such as root mean square error (RMSE), normalized root mean square error (nRMSE), mean absolute error (MAE), mean arctangent absolute percentage error (MAAPE) are used to evaluate performance of the LSTM models. Finally, we found the LSTM model which has the highest prediction accuracy.

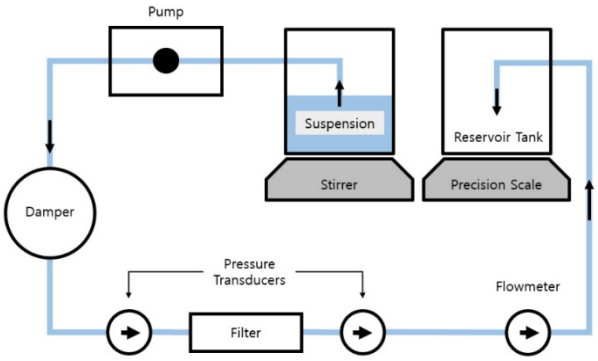

(a) Simplified schematic of the experimental rig

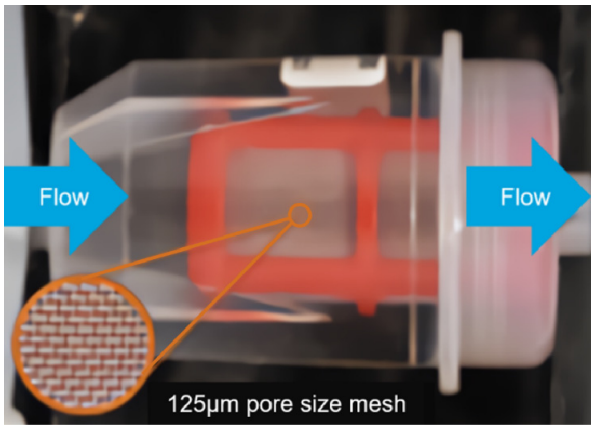

(b) Filter under study

Fig. 1. Description of target system.

The remainder of this paper is organized as follows. Sec. 2 introduces the liquid filtration system and data used in this paper. Sec. 3 describes the main research methods and methodologies. Sec. 4 presents our research process and results. Sec. 5 concludes the paper and suggests directions for future studies.

2. Description of target system and data

Fig. 1 shows the liquid filtration system from which the data used in this study were extracted. The system consists of pump, liquid tanks, damper, filter, pressure and flow rate sensors, and a data acquisition system connected to a computer. An experimental rig uses the pump to flow liquid from one tank to another. The damper prevents tube expansion due to in-

creased pressure in the system. The sensor monitors the flow rate and liquid pressure before and after the filter. The suspension consists of polyetheretherketone (PEEK) particles and water. PEEK particles have a density (1.3 g/cm^3) close to that of water at room temperature and have an extremely low water absorption level (0.1 %/24 h, ASTM D570). The low water absorption level prevents the particles from swelling when mixing with water. Therefore, if the density of the particles is closer to that of water, they can be suspended longer in water.

This research uses filter clogging data of the liquid filter system collected through the experimental equipment mentioned above. The data provided by the PHMe20 Data Challenge include information from the start of the filter until failure. As shown in Table 1, the data can be divided into six groups according to the combination of two variables (particle size and solid ratio), and four experiments were conducted for each group.

Consequently, a total of 24 data files are provided, in which each data file includes three variables (flow rate, upstream pressure, and downstream pressure) measured every 0.1 s. The description of variables is as follows:

- Particle size (micron): Size of PEEK particles used in liquid filter systems
- Solid ratio (%): Percentage of PEEK particles in the liquid passing through the filter
- Flow rate (ml/m): Flow rate of liquid passing through the filter
- Upstream/downstream pressure (PSI): Hydraulic pressure before and after the liquid reaches the filter

Table 1. Operation profiles of samples.

Data group number	Sample data	Particle size (micron)	Solid ratio (%)
1	01-04	45-53	0.4
2	05-08	45-53	0.425
3	09-12	45-53	0.45
4	33-36	63-75	0.4
5	37-40	63-75	0.425
6	41-44	63-75	0.45

The PHMe20 Data Challenge considered a filter to be clogged if the pressure drop is greater than 20, which indicates failure of the filter. A new variable “pressure drop” is the difference between the upstream and downstream pressure. Fig. 2 shows the pressure drop distribution for all sample data.

3. Research method

This research applies a data-driven model to the liquid filter and applies filter failure prognostics. HI is derived by integrating various variables obtained through the sensors connected to the filter, and the health condition of the filter is evaluated using K-means clustering. Furthermore, the HI and RUL are predicted using the LSTM after the performance degradation point. The following is a description of the main methodologies used in this study.

3.1 Division of health stages

Because the change in the HI value is small when the system starts operating, it is difficult to accurately estimate the RUL if the system performance is not degraded [22]. Thus, to estimate the RUL, a process of classifying the health stage using the HI of the system and identifying a point of degradation is required. The health stage pertains to the life cycle or degradation of the health condition of the system, which is generally divided into two or more stages [23].

We use K-means clustering to classify the health stage. K-means clustering is a method of generating an arbitrary number of clusters and assigning each data to the nearest cluster [24]. This method is often used to classify the health stage in the PHM. Cheng et al. (2018) [25] used K-means clustering and divided the health stage of the bearing into four clusters. Siegel and Lee (2011) [26] used K-means clustering to distinguish the health stage of an anemometer.

It is important to determine the optimal number of clusters for accurately evaluating the condition of the system. In this study, the number of clusters was determined using elbow method, which calculates the sum of square error (SSE) while setting

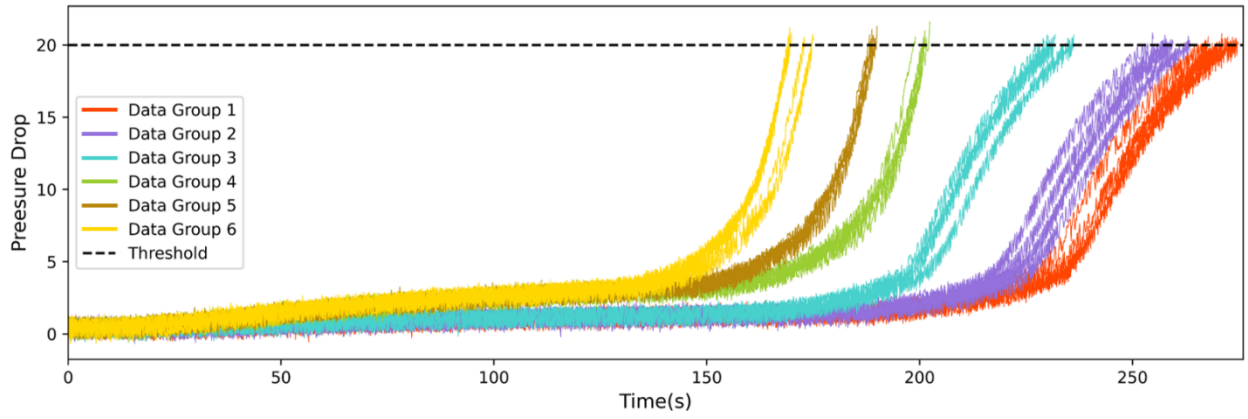

Fig. 2. Distribution of pressure drop.

the number of clusters (K) to 1 and increasing K. The SSE uses the center point of the cluster and other data in each cluster, and the elbow point can be identified based on the rate of change of the SSE according to K. Before a certain value of K, the SSE decreases rapidly, but a subsequent SSE maintains a small rate of change even as K increases. The point representing this trend is defined as the elbow point, and the corresponding K value is the optimal number of clusters [27].

3.2 RUL measurement using HI prediction

In this paper, among the health stages classified through clustering, the stage that shows a definite performance decrease is defined as an unhealthy stage. HI prediction is performed from the starting point of the unhealthy stage. The point where the predicted value of the HI converges or reaches zero is defined as the end of life (EOL) point. We applied the LSTM to predict the HI of the filter up to this point.

LSTM is derived from an RNN, which is often used to predict time-series data. An RNN stores information for learning in the hidden state, but if the initial information is used after a long time, the learning ability is significantly reduced. To consider this problem, cell state was added to the LSTM [28]. Fig. 3 shows the structure of the LSTM cell. Unlike the RNN, the LSTM transfers not only the hidden state but also the cell state to the next step. Since the information of the input is selectively received by using the layer and operation inside the cell, the information of the cell state can be maintained or modified. The complex structure of the LSTM can compensate for the long-term dependency problem that information is lost in a long sequence. The LSTM can be used in various forms as the structure of the cell changes [29].

In the prognostics area of the PHM, various studies have been conducted using LSTM. Yuan et al. (2016) [30] and Wang et al. (2018) [31] used a GRU LSTM and a bidirectional LSTM, respectively, to predict the RUL of an aircraft engine. Wang et al. (2020) [32] predicted the RUL of the fuel cell using a stacked LSTM. In the present study, the HI of the filter is predicted using the following three LSTMs, and the RUL is calculated by identifying the EOL.

- Vanilla LSTM: A basic LSTM model in which the LSTM is composed of a single layer
- Stacked LSTM: LSTM composed of multiple layers
- Bi-directional LSTM: LSTM learning in both forward and reverse directions

The RUL of a filter can be calculated as the difference between the time of measurement and the EOL. The RUL is given as Eq. (1):

$$RUL_{(n)} = t_{(EOL)} - t_{(n)} . \quad (1)$$

In Eq. (1), $t_{(EOL)}$ and $t_{(n)}$ are the time of the EOL and time of the measurement, respectively. The RUL at the current time can be derived by calculating the difference between the EOL and the current time.

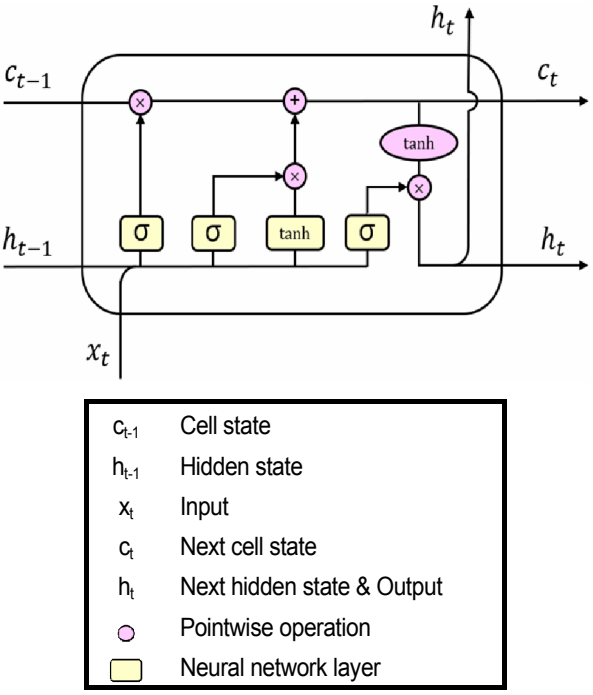

Fig. 3. LSTM cell structure and meaning of elements inside.

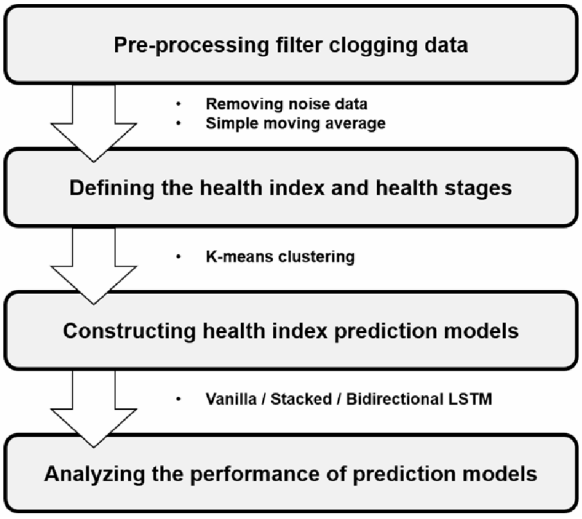

Fig. 4. Flowchart of research.

4. Procedure and results

Fig. 4 shows the procedure of the proposed approach. The first step involves removing noise data and reducing the large deviation in the pressure drop. The HI is then defined, and the health stages are divided using K-means clustering. Subsequently, the HI is predicted using three LSTMs, and thereby the RUL is measured. Finally, the prediction model is verified based on the metrics of the prediction result, and the optimal

LSTM models for predicting the RUL of the liquid filter are identified.

4.1 Pre-processing data

First, the large amount of noise data contained in the data collected by sensors [33] is removed to obtain a meaningful analysis. As shown in Fig. 5, after the initial operation of the filtration system, the initial flow rate is much smaller than the subsequent operation; the initial operation period seems the time until the system entered full-operation mode. Therefore, the data at the front where the flow rate is abnormally small were judged to be noise data and were deleted. In addition, regions with a pressure drop of 20 or more were considered unnecessary due to the continuous measurement of the data after a filter failure.

Values measured at similar times are likely to have similar health states. The data used in this study were measured every 0.1 s, but the deviation in the measured values was extremely large, as shown in Fig. 6. This deviation can cause a miscomprehension that the health of the filter changes rapidly at a similar time and mean that the data contains a lot of noise. Because the pressure drop can deviate significantly, it is difficult to represent the current state of the filter. Accordingly, to improve the stability and accuracy of prediction, the deviation needs to be alleviated. Thus, the moving averaged pressure drop (MAPD) was derived by applying the simple moving average to the pressure drop to reduce any deviation. MAPD is defined as Eq. (2):

$$MAPD_{(t)} = \frac{\sum_{i=0}^{k} PD_{(t-i)}}{k+1} . \quad (2)$$

The simple moving average method continuously calculates the average while moving a fixed size subset. Because the moving average clearly reflects the overall change, it was applied to determine the health states in the filter data. Here, $MAPD_{(t)}$ represents the pressure drop applied with the moving average method at time t and is the average of the pressure drop in a k+1 time series section, from t-k to t. If MAPD is 0, the upstream and downstream pressure are the same, which means that the filter condition is the best. In this study, the optimal value of k was set to 6 through several experiments, and the average value of seven time-series sections was obtained. According to the filter failure criteria mentioned in Sec. 2, the MAPD of 20 indicates failure of the filter.

4.2 Defining the HI and health stages

Indicators that employ various sensor technologies can be used to identify degradation in filter performance. In particular, it is common to utilize the pressure difference before and after the fluid passes through the filter [34]. Therefore, the HI, which scales the MAPD to a value between zero and 1, was derived.

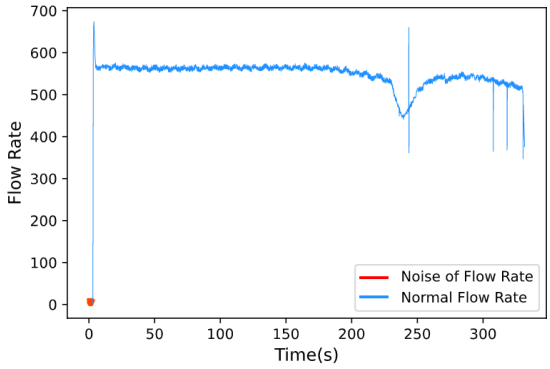

Fig. 5. Detection of noise data using flow rate.

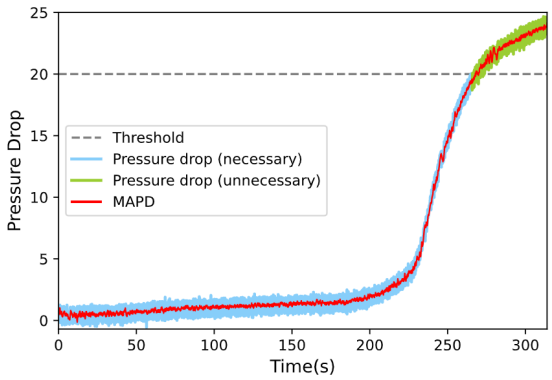

Fig. 6. Detection of noise data.

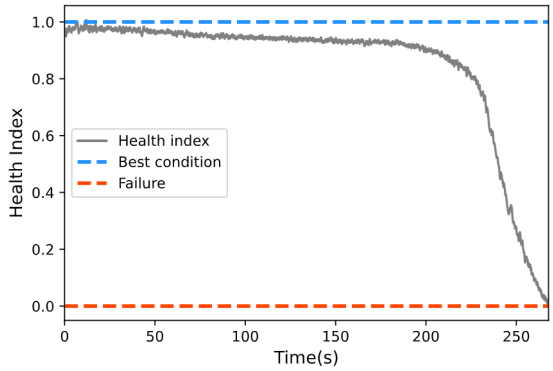

Fig. 7. Health index distribution.

Through the HI, even non-experts who were unaware of the failure criteria of the filter could check its condition. The HI is given as Eq. (3):

$$HI_{(t)} = 1 - \frac{MAPD_{(t)}}{20} . \quad (3)$$

Fig. 7 shows a graph of the HI distribution. The time at which the HI equals 1 is defined as the optimum condition, and the time at which the HI reaches or converges at zero is the EOL. Consequently, the HI at a given point in time is the state of health of the filter at that time.

Most of the HI is concentrated in the healthy or transitional

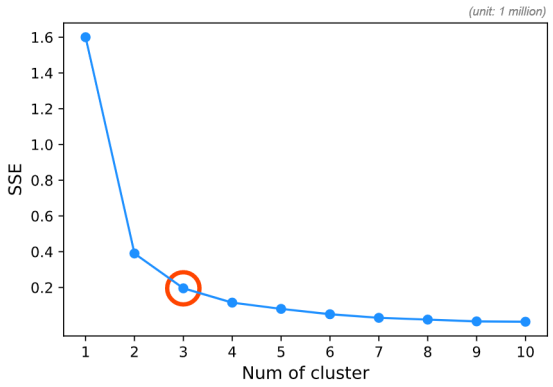

Fig. 8. SSE value and elbow point.

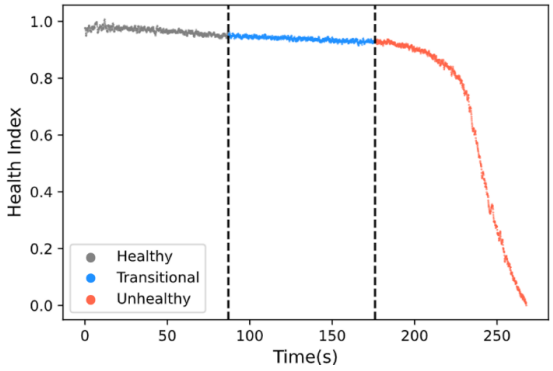

Fig. 9. Division of health stages using K-means clustering.

stage. When the filter is operating normally, the amount of change in the HI is small and difficult to predict. Thus, it is unreasonable to predict prior to reaching the degradation point of the filter [35]. Accordingly, the health stages need to be divided by finding the degradation point, where the filter does not operate normally. In this study, the health stage can be classified using the K-means algorithm and elbow method mentioned in Sec. 3.1. Fig. 8 shows the SSE according to K. Until K reaches 3, the rate of change of the SSE decreases rapidly to 74.9 % and 13.8 %, but thereafter, the rate of change remains stable at less than 5 %. Consequently, the point where K is 3 can be an elbow point. The elbow point of all the experimental data was determined to be 3. Thus, the number of clusters was unified to 3, and K-means clustering was performed. Fig. 9 shows the result of clustering for HI for the first set of experimental data. The health stages were classified into the healthy, transitional, and unhealthy stages.

We defined the boundary between the transitional stage and unhealthy stage as the degradation point. Thus, HI was predicted from the beginning of the unhealthy stage to EOL.

4.3 RUL measurement via HI prediction

The RUL of a machine is the time from the point of measurement to the point at which the machine is determined to have failed. Because the RUL is difficult to predict when the filter is operating normally, it is reasonable to predict during the unhealthy stage. To derive the RUL, the HI was predicted using the LSTM.

The input of the LSTM is a sequence that involves the HI of the past 30 time-series sections including the current time point (t). The output is the HI of the next time point (t+1).

- Input sequence: $[HI_{(t-29)}, HI_{(t-28)}, \ldots, HI_{(t)}]$
- Output value: $HI_{(t+1)}$

The HI of the degradation point defined through clustering is designated as a threshold. If all values of the input sequence are lower than the threshold, the current filter can be determined to be an unhealthy stage. The prediction starts when the input HI sequence is in the unhealthy stage, and the result of the last prediction is added back to the input.

- Input sequence: $[HI_{(t-28)}, HI_{(t-27)}, \ldots, HI_{(t)}, HI_{(t+1)}]$
- Output value: $HI_{(t+2)}$

Consequently, RUL can be estimated by measuring the difference between the time when HI prediction starts and the time when the HI prediction value reaches zero.

In this study, vanilla, stacked, and bidirectional LSTMs were used as the prediction models. These types of LSTM are mainly used in the failure prognostics of the PHM. For a higher prediction accuracy, we iteratively adjusted the parameter values in the LSTM and checked metrics values about predictive model.

Among the several metrics for evaluating the performance of a predictive model, we used four metrics: RMSE, nRMSE, MAE, and MAPE. First, the RMSE is the standard deviation of the prediction error and measures the variance of the residuals. The RMSE is given as follows:

$$RMSE = \sqrt{\frac{1}{n}\sum_{1}^{n}\left(X_{real} - X_{pred}\right)^2} . \quad (4)$$

The nRMSE normalizes the RMSE to match the units of each model, to ensure that the models are comparable. The nRMSE is given as follows:

$$nRMSE = \frac{RMSE}{avg\left(X_{real}\right)} . \quad (5)$$

The MAE is the average of the absolute difference between the predicted and actual values for all instances in the test data. All individual differences are considered equal weight and MAE is given as follows:

$$MAE = \frac{1}{n}\sum_{1}^{n}\left|X_{real} - X_{pred}\right| . \quad (6)$$

Lastly, MAPE is a frequently used metric to evaluate predictive performance. However, if the actual value is 0, the MAPE cannot be calculated, and if the actual value is less than 1, the

Table 2. Optimal parameters of HI prediction.

Data group number	Training data	Test data	Threshold	LSTM model	Learning rate	Epoch	Dropout	Hidden node
1	01-03	04	0.929286	Vanilla	0.001	162	0	32
				Stacked	0.001	210	0.1	16
				Bidirectional	0.001	210	0	60
2	05-07	08	0.928482	Vanilla	0.001	162	0	32
				Stacked	0.001	210	0	16
				Bidirectional	0.001	210	0	60
3	09-11	12	0.925179	Vanilla	0.001	162	0	32
				Stacked	0.001	150	0.1	161
				Bidirectional	0.001	162	0	60
4	33-35	36	0.852947	Vanilla	0.001	162	0	32
				Stacked	0.001	150	0	16
				Bidirectional	0.001	210	0	64
5	37-39	40	0.850569	Vanilla	0.001	210	0	32
				Stacked	0.001	210	0	16
				Bidirectional	0.001	210	0	32
6	41-43	44	0.847221	Vanilla	0.001	210	0	32
				Stacked	0.001	210	0	16
				Bidirectional	0.001	210	0	64

Table 3. Performance metrics of HI prediction.

Data group number	Training data	Test data	Threshold	LSTM model	RMSE (%)	nRMSE (%)	MAE (%)	MAAPE (%)
1	01-03	04	0.929286	Vanilla	3.189	5.074	2.428	9.464
				Stacked	3.198	5.432	2.869	12.145
				Bidirectional	3.376	5.742	2.682	7.231
2	05-07	08	0.928482	Vanilla	2.494	4.264	1.915	7.707
				Stacked	3.096	5.293	2.454	7.473
				Bidirectional	1.134	1.938	0.797	4.054
3	09-11	12	0.925179	Vanilla	4.023	6.198	3.357	10.728
				Stacked	4.113	6.337	3.561	10.319
				Bidirectional	3.366	5.076	2.948	8.252
4	33-35	36	0.852947	Vanilla	2.158	3.212	1.840	3.764
				Stacked	3.427	5.324	2.808	6.623
				Bidirectional	4.712	7.100	4.246	10.375
5	37-39	40	0.850569	Vanilla	3.874	5.872	2.732	6.067
				Stacked	4.044	6.023	3.250	7.694
				Bidirectional	4.100	6.083	3.182	7.505
6	41-43	44	0.847221	Vanilla	2.698	4.329	2.090	6.159
				Stacked	2.390	3.952	1.641	7.827
				Bidirectional	1.294	2.105	0.916	3.408

MAPE has a value close to infinity. To solve the aforementioned problem of MAPE, Kim and Kim (2016) [36] proposed a new prediction accuracy metric called MAAPE. Because all the actual value of HI used in the predictive model were less than 1, this study used MAAPE. This metric is given as follows:

$$MAAPE = \frac{1}{n}\sum_{1}^{n}\left(\arctan\left(\left|\frac{X_{real}-X_{pred}}{X_{real}}\right|\right)\right). \quad (7)$$

In this paper, LSTM models were created for all six data

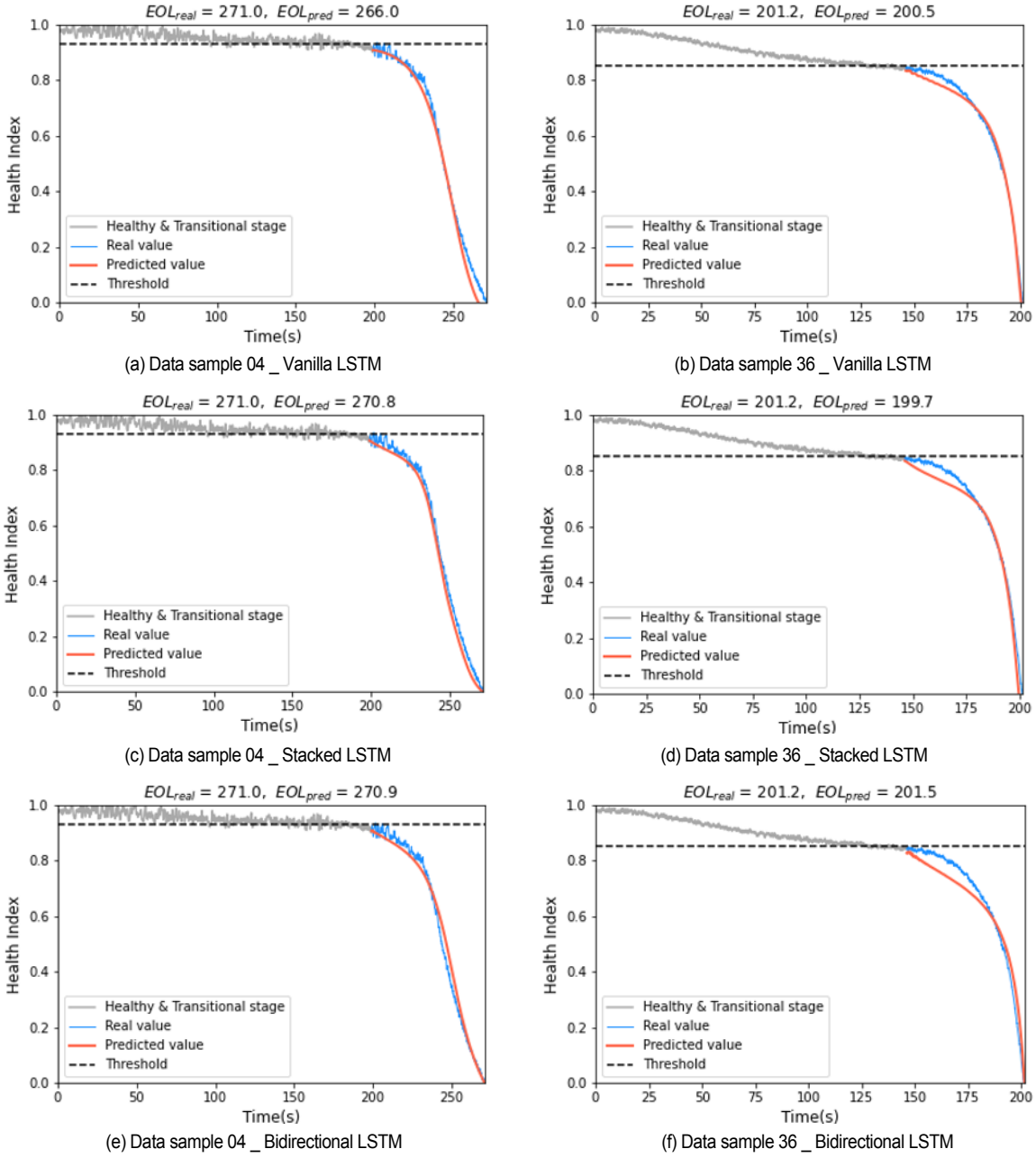

(a) Data sample 04 _ Vanilla LSTM

(b) Data sample 36 _ Vanilla LSTM

(c) Data sample 04 _ Stacked LSTM

(d) Data sample 36 _ Stacked LSTM

(e) Data sample 04 _ Bidirectional LSTM

(f) Data sample 36 _ Bidirectional LSTM

Fig. 10. Examples of RUL estimation results (data sample 04 & 36).

groups. Experiments were conducted by repeatedly changing all parameters. The optimal model under each group was chosen as the model with the smallest of the three metrics values obtained from the actual HI and the predicted HI of the test data. During the learning step, the activation function was Elu, the batch size used for training was 1, and the optimizer was Kingma and Adam [37].

Tables 2 and 3 shows the optimal parameters and performance metrics of the three LSTM models regarding the HI prediction with the test data. Among the parameters in the table, the learning rate controls the rate at which the model adapts to the problem. If learning rate has low value, requires more training epochs because change less weights in each update, whereas high learning rate results rapid changes and requires fewer training epochs. Epoch refers to the number of times it has learned over the entire data set. Dropout means temporarily removing units (hidden and visible) from the neural network along with all incoming and outgoing connections. This parameter is used to avoid the overfitting problems. Lastly, hidden node is a dimensionality of the output space. This study used grid search method to find the optimal combination of various hyperparameter values. In the grid search, the hyperparameter range is set, and parameter values are assigned at regular intervals within the range to select the variable value represent-

Table 4. Performances of the LSTM models.

LSTM model	RMSE	nRMSE	MAE	MAAPE
Vanilla	3.073	4.825	**2.394**	7.315
Stacked	3.378	5.394	2.764	8.680
Bidirectional	**2.997**	**4.674**	2.462	**6.804**

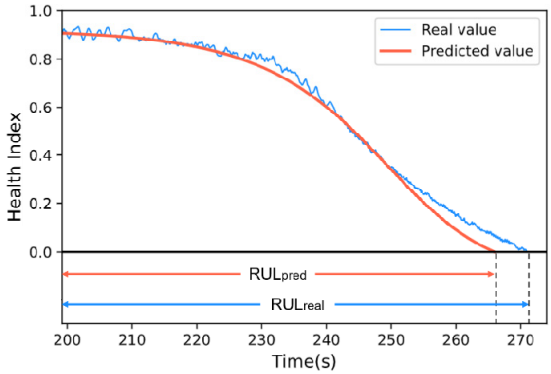

Fig. 11. RUL measurement through HI prediction (data sample 04, Vanilla LSTM).

ing the best experimental result. In data groups 1, 4 and 5 the vanilla LSTM showed optimum performance for the test data. And the bidirectional LSTM applied to groups 2, 3 and 6 performed the best. Fig. 10 shows the HI prediction results and indicates that the difference between the actual EOL and the predicted EOL is not large. Therefore, at the degradation point, the actual RUL and the predicted RUL are also similar (Fig. 11).

Finally, we computed and compared each metrics' average of four metrics (Table 4). Consequently, it can be seen the bidirectional LSTM has the highest prediction accuracy.

5. Conclusions

Filters are important for the smooth operation of mechanical systems in various industries. Accordingly, various PHM studies have been conducted on the RUL prediction of filters. However, studies on liquid filters have been insufficient compared to studies on other filter types. Moreover, studies in this area have primarily focused on physics-based models.

In this study, health condition and RUL prognosis based on sensor data of a liquid filter was conducted. The HI of the filter was defined, and the degradation point of the performance was identified through K-means clustering. After predicting the unhealthy stage of HI with three LSTM models, four metrics were used to evaluate the performance of the models. Furthermore, a comparison the metrics' average of the three LSTM models showed that the bidirectional LSTM achieved the best performance. Therefore, it can be stated that the data-driven prognostics of the RUL using bidirectional LSTM is an effective method for the maintenance of a liquid filter.

We defined and predicted the HI as an indicator that integrates the various properties and environments of liquid filters. It contributes to the evaluation of the current condition of a target system as well as the RUL prognostics based on the HI prediction data. In addition, a generic approach that can be applied to various types of liquid filters was developed using data that included only the characteristics of a typical liquid filter. Therefore, this study is expected to contribute to the maintenance for the smooth operation of various liquid filters.

Future studies may advance the HI and RUL prognosis of liquid filters through a hybrid drive model that incorporates both a physics-based model and a data-driven model.

Acknowledgments

This work was supported by the Human Resources Program in Energy Technology of the Korea Institute of Energy Technology Evaluation and Planning (KETEP), the Ministry of Trade, Industry and Energy (MOTIE) of the Republic of Korea (No. 20204010600220). This work was supported by the National Research Foundation of Korea (NRF) grant funded by the Korea government (MSIT) (2019R1A2C1090228).

References

[1] O. F. Eker, F. Camci and I. K. Jennions, Physics-based prognostic modelling of filter clogging phenomena, *Mechanical Systems and Signal Processing*, 75 (2016) 395-412.

[2] R. Kristiansen, Sand-filter trenches for purification of septic tank effluent: I. The clogging mechanism and soil physical environment, *Journal of Environmental Quality*, 10 (3) (1981) 353-357.

[3] A. Grall, C. Bérenguer and L. Dieulle, A condition-based maintenance policy for stochastically deteriorating systems, *Reliability Engineering and System Safety*, 76 (2) (2002) 167-180.

[4] J. Zhang and J. Lee, A review on prognostics and health monitoring of Li-ion battery, *Journal of Power Sources*, 196 (15) (2011) 6007-6014.

[5] X. Jia, C. Jin, M. Buzza, Y. Di, D. Siegel and J. Lee, A deviation based assessment methodology for multiple machine health patterns classification and fault detection, *Mechanical Systems and Signal Processing*, 99 (2018) 244-261.

[6] G. W. Vogl, B. A. Weiss and M. Helu, A review of diagnostic and prognostic capabilities and best practices for manufacturing, *Journal of Intelligent Manufacturing*, 30 (1) (2019) 79-95.

[7] O. Fink, Q. Wang, M. Svensén, P. Dersin, W.-J. Lee and M. Ducoffe, Potential, challenges and future directions for deep learning in prognostics and health management applications, *Engineering Applications of Artificial Intelligence*, 92 (2020) 103678.

[8] X. Jia, B. Huang, J. Feng, H. Cai and J. Lee, A review of PHM data competitions from 2008 to 2017: methodologies and analytics, *Proceedings of the Annual Conference of the Prognostics and Health Management Society* (2018).

[9] X.-S. Si, W. Wang, C.-H. Hu and D.-H. Zhou, Remaining

useful life estimation-a review on the statistical data driven approaches, *European Journal of Operational Research*, 213 (1) (2011) 1-14.

[10] R. Khelif, B. Chebel-Morello, S. Malinowski, E. Laajili, F. Fnaiech and N. Zerhouni, Direct remaining useful life estimation based on support vector regression, *IEEE Transactions on Industrial Electronics*, 64 (3) (2016) 2276-2285.

[11] A. Cubillo, S. Perinpanayagam and M. Esperon-Miguez, A review of physics-based models in prognostics: application to gears and bearings of rotating machinery, *Advances in Mechanical Engineering*, 8 (8) (2016) 1687814016664660.

[12] J. Qiu, B. B. Seth, S. Y. Liang and C. Zhang, Damage mechanics approach for bearing lifetime prognostics, *Mechanical Systems and Signal Processing*, 16 (5) (2002) 817-829.

[13] R. Zhao, J. Wang, R. Yan and K. Mao, Machine health monitoring with LSTM networks, *2016 10th International Conference on Sensing Technology (ICST),* IEEE (2016).

[14] Y. Lei, N. Li, L. Guo, N. Li, T. Yan and J. Lin, Machinery health prognostics: a systematic review from data acquisition to RUL prediction, *Mechanical Systems and Signal Processing*, 104 (2018) 799-834.

[15] A. Elsheikh, S. Yacout and M.-S. Ouali, Bidirectional handshaking LSTM for remaining useful life prediction, *Neurocomputing*, 323 (2019) 148-156.

[16] A. Nuhic, T. Terzimehic, T. Soczka-Guth, M. Buchholz and K. Dietmayer, Health diagnosis and remaining useful life prognostics of lithium-ion batteries using data-driven methods, *Journal of Power Sources*, 239 (2013) 680-688.

[17] Z. Skaf, O. F. Eker and I. K. Jennions, A simple state-based prognostic model for filter clogging, *Procedia CIRP*, 38 (2015) 177-182.

[18] S.-L. Ho, M. Xie and T. N. Goh, A comparative study of neural network and Box-Jenkins ARIMA modeling in time series prediction, *Computers and Industrial Engineering*, 42 (2-4) (2002) 371-375.

[19] T. J. Phelps, A. V. Palumbo, B. Bischoff, C. Miller, L. Fagan, M. McNeilly and R. R. Judkins, Micron-pore-sized metallic filter tube membranes for filtration of particulates and water purification, *Journal of Microbiological Methods*, 74 (1) (2008) 10-16.

[20] A. Jahromi, R. Piercy, S. Cress, J. Service and W. Fan, An approach to power transformer asset management using health index, *IEEE Electrical Insulation Magazine*, 25 (2) (2009) 20-34.

[21] Y. Wu, M. Yuan, S. Dong, L. Lin and Y. Liu, Remaining useful life estimation of engineered systems using vanilla LSTM neural networks, *Neurocomputing*, 275 (2018) 167-179.

[22] J. Shi, Y. Li, G. Wang and X. Li, Health index synthetization and remaining useful life estimation for turbofan engines based on run-to-failure datasets, *Eksploatacja i Niezawodność*, 18 (4) (2016).

[23] O. O. Aremu, D. Hyland-Wood and P. R. McAree, A relative entropy weibull-sax framework for health indices construction and health stage division in degradation modeling of multivariate time series asset data, *Advanced Engineering Informatics*, 40 (2019) 121-134.

[24] K. Xing, C. Hu, J. Yu, X. Cheng and F. Zhang, Mutual privacy preserving k-means clustering in social participatory sensing, *IEEE Transactions on Industrial Informatics*, 13 (4) (2017) 2066-2076.

[25] Y. Cheng, J. Peng, X. Gu, X. Zhang, W. Liu, Y. Yang and Z. Huang, RLCP: A reinforcement learning method for health stage division using change points, *2018 IEEE International Conference on Prognostics and Health Management (ICPHM)*, IEEE (2018).

[26] D. Siegel and J. Lee, An auto-associative residual processing and K-means clustering approach for anemometer health assessment, *International Journal of Prognostics and Health Management,* 2 (2011) 117.

[27] P. Bholowalia and A. Kumar, EBK-means: a clustering technique based on elbow method and k-means in WSN, *International Journal of Computer Applications*, 105 (9) (2014).

[28] S. Selvin, R. Vinayakumar, E. Gopalakrishnan, V. K. Menon and K. Soman, Stock price prediction using LSTM, RNN and CNN-sliding window model, *2017 International Conference on Advances in Computing, Communications and Informatics (ICACCI),* IEEE (2017).

[29] D. Thara, B. PremaSudha and F. Xiong, Epileptic seizure detection and prediction using stacked bidirectional long short term memory, *Pattern Recognition Letters*, 128 (2019) 529-535.

[30] M. Yuan, Y. Wu and L. Lin, Fault diagnosis and remaining useful life estimation of aero engine using LSTM neural network, *2016 IEEE International Conference on Aircraft Utility Systems (AUS)*, IEEE (2016).

[31] J. Wang, G. Wen, S. Yang and Y. Liu, Remaining useful life estimation in prognostics using deep bidirectional lstm neural network, *2018 Prognostics and System Health Management Conference (PHM-Chongqing),* IEEE (2018).

[32] F.-K. Wang, X.-B. Cheng and K.-C. Hsiao, Stacked long short-term memory model for proton exchange membrane fuel cell systems degradation, *Journal of Power Sources*, 448 (2020) 227591.

[33] L.-M. Ang, K. P. Seng, A. M. Zungeru and G. K. Ijemaru, Big sensor data systems for smart cities, *IEEE Internet of Things Journal*, 4 (5) (2017) 1259-1271.

[34] S. Calle, P. Contal, D. Thomas, D. Bémer and D. Leclerc, Evolutions of efficiency and pressure drop of filter media during clogging and cleaning cycles, *Powder Technology*, 128 (2-3) (2002) 213-217.

[35] F. O. Heimes, Recurrent neural networks for remaining useful life estimation, *2008 International Conference on Prognostics and Health Management,* IEEE (2008).

[36] S. Kim and H. Kim, A new metric of absolute percentage error for intermittent demand forecasts, *International Journal of Forecasting*, 32 (3) (2016) 669-679.

[37] D. P. Kingma and J. Ba, Adam: a method for stochastic optimization, *arXiv preprint arXiv:1412.6980* (2014).

Seunghyun Lee was born in Suwon, South Korea in 1996. He received the B.S. degrees in industrial engineering at Konkuk University, Seoul, South Korea, in 2021. He is currently working toward the M.S. degree in industrial engineering at Konkuk University, Seoul, South Korea. His research interests include data-driven prognostics and health management, social media mining for business opportunity discovery, and data mining for product/equipment monitoring.

Seungju Lee was born in Seoul, South Korea in 1996. His research interests include data-driven prognostics and health management and software development.

Kwonneung Lee was born in Seoul, South Korea in 1995. His research interests include data-driven prognostics and health management, statistical data analysis, and machine learning.

Sangwon Lee was born in Gumi, South Korea in 1996. His research interests include data-driven prognostics and health management and computer algorithms.

Jaemin Chung was born in Seoul, South Korea in 1995. He received the B.S. degrees in industrial engineering at Konkuk University, Seoul, South Korea, in 2020. He is currently working toward the M.S. degree in industrial engineering at Konkuk University, Seoul, South Korea. His research interests include patent/social media mining for business opportunity discovery and data-driven prognostics and health management.

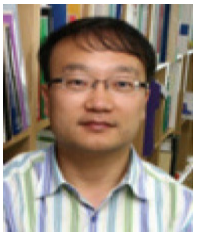

Chang-Wan Kim was born in Pohang, South Korea in 1969. He received a B.S. degree in mechanical engineering, Hanyang University, Seoul, South Korea in 1987. He received an M.S. degree in mechanical engineering, Pohang University of Science and Technology, Pohang, South Korea in 1993. He received an M.S. degree in computational applied mathematics, and a Ph.D. in aerospace and engineering mechanics, University of Texas at Austin, Texas, USA, in 1997 and 1999, respectively. He is currently a Professor at the Department of Mechanical Engineering, Konkuk University, Seoul, South Korea. His research interests include vibration and noise analysis, multi-body dynamics, finite element analysis, and multi-physics system analysis.

Janghyeok Yoon was born in Daegu, South Korea in 1979. He received B.S. and M.S. degrees and a Ph.D. in industrial engineering at Pohang University of Science and Technology, Pohang, South Korea in 2002, 2004, and 2011, respectively. He has industrial experience at companies and research institutes such as LG and Korea Institute of Intellectual Property. He is currently an Associate Professor at the Department of Industrial Engineering, Konkuk University, Seoul, South Korea. His research interest is in technology intelligence-related topics, including technology forecasting, technology opportunity identification, technology road mapping, technology convergence, and business intelligence, including social media mining.